

## Flow field disturbance due to point viscosity variations in a heterogeneous fluid

Debasish Das <sup>\*</sup>*Department of Mathematics and Statistics, University of Strathclyde, 26 Richmond Street, Glasgow G1 1XH, Scotland, United Kingdom*

(Received 24 March 2022; accepted 12 April 2023; published 8 May 2023)

We derive the flow field disturbance produced by point viscosity variations in a heterogeneous fluid when subject to a background flow while neglecting fluid inertia. The disturbance flow field is found to be identical to that generated by a force dipole called a stresslet. Using a combination of theory and numerical simulations, we show how the hydrodynamics of an active rigid particle is altered due to the presence of point viscosity variations, and how this can be exploited to manipulate and steer them in microfluidic environments.

DOI: [10.1103/PhysRevFluids.8.L051301](https://doi.org/10.1103/PhysRevFluids.8.L051301)

Fluids encountered in nature and industry are usually heterogeneous. For example, blood is composed of plasma, red and white blood cells, and platelets. The plasma itself is heterogeneous as it is an aqueous solution containing organic molecules, proteins, and salts [1]. Similarly, interstitial fluid in solid tumors is a highly disordered environment when compared to normal tissues which has significant consequences on nanomedicine delivery [2,3]. The cytoplasmic matrix is mostly an aqueous environment but made heterogeneous due to the presence of various macromolecules. More recently, it has been discovered that cells contain numerous membraneless compartments that exhibit liquidlike behavior [4,5]. Examples include nucleolus and Cajal bodies in the nucleus, and P-bodies, stress and germ granules in the cytoplasm [6]. It has also been reported that P-bodies dispersed within the cytoplasm have much higher viscosity,  $\sim 1.0$  Pa s, than their surroundings. Hence, naturally the question arises: How do we model such heterogeneous fluids encountered frequently in biology? Heterogeneous fluids are also abundantly found in various industrial settings. Many manufacturing processes involve transportation and filling of polymeric materials in channels [7,8]. These processes usually require the fluid to remain homogeneous at all times but deviations occur due to impurities, segregation of different polymeric constituents, or geometrical imperfections in the transportation channel, making the effective fluid viscosity spatially heterogeneous.

A fluid can be heterogeneous in either its density or viscosity—its two basic material properties. In this Letter, we focus on viscosity variations of the fluid while assuming that its density remains unchanged in space and time. A few papers have considered the effect of variable viscosity on flows in parallel [9–11], converging and diverging channels [12], and on the motion of a hot sphere [13,14]. However, a fundamental fluid mechanical question has remain unaddressed: How is an ambient flow field disturbed due to a point viscosity variation in the fluid? If we are able to answer

---

\*debasish.das@strath.ac.uk

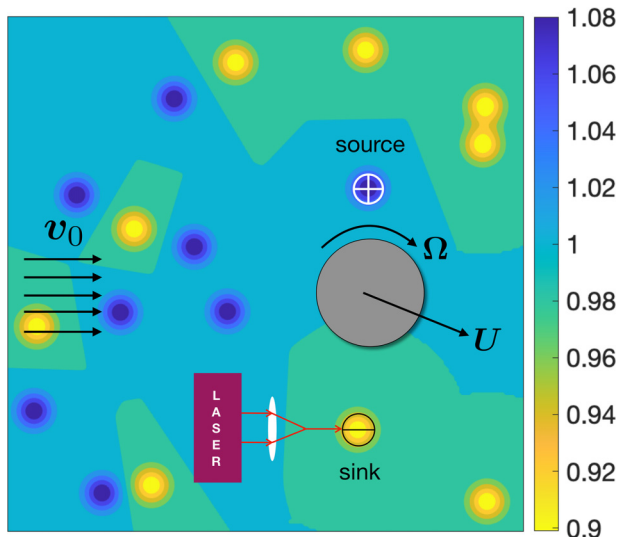


FIG. 1. An illustrative example of a heterogeneous fluid with arbitrarily varying viscosity in space,  $\mu(\mathbf{x})$ , modeled as discrete viscosity sources (blue,  $\oplus$ ) and sinks (yellow,  $\ominus$ ) of appropriate strengths interacting with a background flow  $\mathbf{v}_0$ . Viscosity sinks or sources may be created in an otherwise homogeneous fluid by locally heating or cooling, respectively. An active rigid particle is shown whose motion is significantly altered due to the presence of point viscosities as its translational,  $\mathbf{U}$ , and rotational,  $\mathbf{\Omega}$ , velocity becomes coupled.

this question, we can create an arbitrary spatial distribution of viscosity discretely by placing viscosity sources and sinks of appropriate strength, allowing us to model many heterogeneous fluids such as those described above. Figure 1 shows an illustrative example where multiple point viscosities may alter the motion of a rigid particle. In situations where an otherwise homogeneous fluid is locally heated or cooled, for example, by the use of laser or spray freezing, the model of point viscosities is directly applicable with the assumption that the timescales of interest are smaller than the timescales at which these point viscosities diffuse, making the problem quasistatic. It is noteworthy that the idea of locally heating fluid has been recently used to artificially create cytoplasmic flows inside *C. elegans* zygotes [15,16].

We restrict ourselves to an inertialess fluid whose dynamics are governed by the Stokes equation [17–19],

$$-\nabla p(\mathbf{x}) + \nabla \cdot [\mu(\mathbf{x})\{\nabla \mathbf{v}(\mathbf{x}) + \nabla \mathbf{v}^T(\mathbf{x})\}] + \mathbf{F}\delta(\mathbf{x} - \mathbf{x}_0) = \mathbf{0}, \quad (1)$$

together with the incompressibility condition  $\nabla \cdot \mathbf{v} = 0$ . Here,  $p$ ,  $\mathbf{v}$  are the fluid pressure and velocity that need to be determined for a given spatial distribution of viscosity  $\mu(\mathbf{x})$  and a point force  $\mathbf{F}$  acting at  $\mathbf{x} = \mathbf{x}_0$ . The base flow  $\mathbf{v}_0$  is generated by a point force or Stokeslet, however, it may also include any background flow. We then prescribe the fluid to have a uniform viscosity  $\mu_0$  everywhere except at certain locations,  $\mathbf{x} = \mathbf{x}_\alpha$ , so that  $\mu(\mathbf{x}) = \mu_0 + \sum_{\alpha=1}^N \mu_\alpha \delta(\mathbf{x} - \mathbf{x}_\alpha)$ ,  $\delta$  being the Dirac delta function [20] and  $N$  being the total number of point viscosities in space. For an arbitrarily varying viscosity in space,  $\mu(\mathbf{x})$ , regions that have higher or lower viscosities than the ambient fluid are represented as concentrated viscosity sources ( $\mu_\alpha > 0$ ) or sinks ( $\mu_\alpha < 0$ ) of appropriate strengths, respectively, as a first approximation. It is noted that since  $\int_{-\infty}^{\infty} \delta(\mathbf{x} - \mathbf{x}_\alpha) d\mathbf{r} = 1$ ,  $\mu_\alpha$  has units of  $[\mu V]$ , where  $V$  is volume. It represents viscosity times the volume of a small region such that their product remains finite. The point viscosity model circumvents the use of computationally expensive volume-discretizing numerical simulations and gives physical insight into the effect of the spatial variations in viscosity on the flow pressure and velocity.

The flow field due to a point viscosity has physical meaning everywhere except at the point where they are present. We use Fourier transforms to solve Eq. (1) by defining  $(p, \mathbf{v}) = (2\pi)^{-3/2} \int_{-\infty}^{\infty} (\hat{p}, \hat{\mathbf{v}}) \exp(i\mathbf{k} \cdot \mathbf{x}) d\mathbf{k}$ , where  $\hat{p}, \hat{\mathbf{v}}$  are the Fourier transforms of  $p, \mathbf{v}$ , respectively. After some algebraic manipulations [see Supplemental Material (SM) [21]], the Stokes equation in the Fourier space reads

$$-i\mathbf{k}\hat{p} - \mu_0 k^2 \hat{\mathbf{v}} + \hat{\mathbf{F}} + (2\pi)^{-3/2} \sum_{\alpha=1}^N [\mu_{\alpha} e^{-i\mathbf{k} \cdot \mathbf{x}_{\alpha}} i\mathbf{k} \cdot [\nabla \tilde{\mathbf{v}}(\mathbf{x}_{\alpha}) + \nabla \tilde{\mathbf{v}}^T(\mathbf{x}_{\alpha})]] = \mathbf{0}, \quad (2)$$

together with  $i\mathbf{k} \cdot \hat{\mathbf{v}} = 0$ . Crucially, we note that we have used the derivative shifting property of the delta function to find Eq. (2) (see Lighthill's monograph [20]). The Fourier transform of the point force is  $\hat{\mathbf{F}} = (2\pi)^{-3/2} \mathbf{F} \exp(-i\mathbf{k} \cdot \mathbf{x}_0)$ . If the velocity is to be evaluated at one of the locations of the point viscosity,  $\mathbf{x} = \mathbf{x}_{\alpha}$ , the leading-order velocity will be due to the point force to which we must add the disturbance velocities from all point viscosities except the one at  $\mathbf{x} = \mathbf{x}_{\alpha}$ . To make this distinction, we have replaced  $\mathbf{v}$  with  $\tilde{\mathbf{v}}$ . However, if the velocity is to be found at any other location,  $\mathbf{x} \neq \mathbf{x}_{0,\alpha}$ , then the net velocity will have contributions from all point viscosities. It is noted that  $\nabla \tilde{\mathbf{v}}(\mathbf{x}) + \nabla \tilde{\mathbf{v}}^T(\mathbf{x}) = 2\mathbf{E}_{\alpha}$  is twice the straining flow at the location of the point viscosity at  $\mathbf{x} = \mathbf{x}_{\alpha}$ . Taking a dot product of Eq. (2) with  $\mathbf{k}$  eliminates  $\hat{\mathbf{v}}$ , and we obtain an equation for  $\hat{p}$ . The pressure field is found by taking the inverse Fourier transform of  $\hat{p}$ ,

$$p = p_0 - \sum_{\alpha=1}^N \frac{3\mu_{\alpha}}{2\pi r_{\alpha}^5} [\mathbf{r}_{\alpha} \mathbf{r}_{\alpha} : (\nabla \tilde{\mathbf{v}})_{\mathbf{x}=\mathbf{x}_{\alpha}}], \quad (3)$$

where  $\mathbf{r}_{\alpha} = \mathbf{x} - \mathbf{x}_{\alpha}$ ,  $\mathbf{r}_0 = \mathbf{x} - \mathbf{x}_0$ , and  $p_0 = \mathbf{F} \cdot \mathbf{r}_0 / 4\pi r_0^3$  is the pressure field due to a Stokeslet. Following a similar procedure, we find the flow field due to a point force, perturbed by point viscosities,

$$\mathbf{v} = \mathbf{v}_0 - \sum_{\alpha=1}^N \frac{3\mu_{\alpha}}{4\pi \mu_0 r_{\alpha}^5} \mathbf{r}_{\alpha} [\mathbf{r}_{\alpha} \mathbf{r}_{\alpha} : (\nabla \tilde{\mathbf{v}})_{\mathbf{x}=\mathbf{x}_{\alpha}}]. \quad (4)$$

The forcing for Eqs. (3) and (4) is the velocity generated by a Stokeslet,

$$\mathbf{v}_0 = \frac{1}{8\pi \mu_0} \mathbf{F} \cdot \mathbf{G}, \quad (5)$$

where

$$\mathbf{G} = \frac{\mathbf{I}}{r_0} + \frac{\mathbf{r}_0 \mathbf{r}_0}{r_0^3}$$

is the Oseen-Burgers tensor. The second terms on the left-hand sides of Eqs. (3) and (4) are the disturbance fields arising from a point viscosity, identical to those arising from a stresslet [18,19]. It is instructive to note that the stresslet due to the point viscosity only acts upon the straining part of the flow field,  $\tilde{\mathbf{v}}$ . For a single isolated point viscosity, Eqs. (3) and (4) are easily solved as  $\tilde{\mathbf{v}} = \mathbf{v}_0$ . However, when multiple point viscosities are present, they interact with each other, and either a coupled system of equations need to be solved numerically or a method of reflections may be used to make analytical progress (see SM [21] for an illustrative example). Henceforth, when considering multiple point viscosities, we only retain the leading-order effect and neglect hydrodynamic interactions between them, i.e.,  $\tilde{\mathbf{v}} = \mathbf{v}_0$ . This is a valid assumption when  $\mu_{\alpha} / \mu_0 L^3$ , i.e. either the viscosity variations are small in magnitude compared with the background viscosity and/or they are well separated from each other,  $L$  being the separation distance.

Remarkably, the flow field in Eq. (4) changes sign with  $\mu_{\alpha}$ . This may seem unphysical when considering Taylor's classic emulsion problem [23] of flow around drops suspended in a fluid. However, the two problems are different. Taylor prescribes a sharp interface between two fluid regions of different viscosity and applies a straining flow. The drop remains spherical at all times

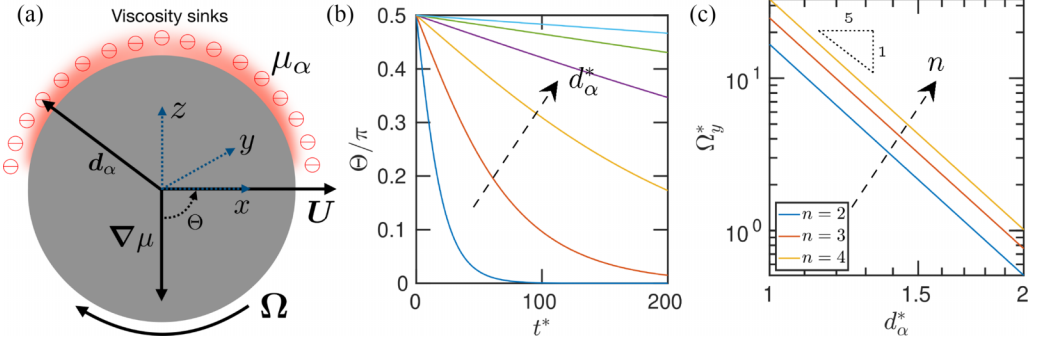


FIG. 2. (a) Schematic diagram of a spherical active particle surrounded by identical viscosity sinks. The viscosity sinks may be generated due to the particle surface being hot, direct heating of the fluid by a laser, or due to secretions from an organism that reduce the viscosity of the surrounding medium. (b) Angle made by the translational velocity of a spherical particle placed next to viscosity sinks at various distances  $d_\alpha^* = d_\alpha/a = 1 - 2$  and the effective viscosity gradient  $\Theta$  plotted as a function of dimensionless time,  $t^* = tU/a$ . All the viscosity sinks are identical, of strength  $\mu_\alpha = -0.01\mu_0$ . Their number is kept fixed at 57 and their number density  $n$  ranges from 1.1 to 4.5 as  $d_\alpha^*$  varies. (c) Log-log plot of dimensionless angular velocity,  $\Omega_y^* = \Omega_y a/U$ , as a function of dimensionless distance between the viscosity sink and sphere's center,  $d_\alpha^*$ , for various number densities  $n$ .

due to strong surface tension. This causes a jump in the pressure across the interface. The final expression for the velocity in that paper does not switch signs when the viscosity of the drop is less or more than the surrounding fluid. In the point viscosity model, there is only one fluid and hence a sharp fluid-fluid interface or surface tension do not exist. The equivalent result for the point viscosity may be derived by prescribing continuity of radial stresses and discarding the kinematic boundary condition. The velocity field obtained in this case is directly proportional to  $\mu_\alpha$ , which is consistent with Eq. (4) (see SM [21]). Furthermore, the point viscosity model can be thought of as the limiting case of a Gaussian viscosity profile as its width vanishes. The changing of sign as the viscosity of the Gaussian profile is higher or lower than ambient fluid is also evidenced in full numerical simulations (see SM [21]). Another key difference between the two problems is that  $\mu_\alpha \rightarrow \infty$  is a singular limit in the point viscosity model while in the Taylor's problem it represents a solid sphere. Next, we consider the canonical case of a spherical active particle whose motion is altered due to the presence of a viscosity sink or a source. We assume that the particle is torque free and has a self-propulsion velocity generated by an internal mechanism. We place a viscosity sink(s) next to one half of the translating sphere [see Fig. 2(a)]. The flow field due to a translating sphere of radius  $a$  located at  $\mathbf{x}_c$ ,

$$\mathbf{v}_0 = \frac{3a}{4}\mathbf{U} \cdot \left[ \left( \frac{\mathbf{I}}{r_c} + \frac{\mathbf{r}_c \mathbf{r}_c}{r_c^3} \right) + a^2 \left( \frac{\mathbf{I}}{3r_c^3} - \frac{\mathbf{r}_c \mathbf{r}_c}{r_c^5} \right) \right], \quad (6)$$

serves as the base flow, where  $\mathbf{r}_c = \mathbf{x} - \mathbf{x}_c$ . In Eq. (6), we have only retained the leading-order velocity flow field and neglected  $O(\mu_\alpha a/\mu_0 d_\alpha^4)$  contributions, where  $\mathbf{d}_\alpha = \mathbf{x}_\alpha - \mathbf{x}_c$ ,  $d_\alpha = |\mathbf{d}_\alpha|$  and  $\hat{\mathbf{d}}_\alpha = \mathbf{d}_\alpha/d_\alpha$ . The first and second terms are associated with flows created by a Stokeslet and source dipole, respectively. The flow due to the translating sphere interacts with the point viscosity sink and creates a disturbance flow around the sphere itself given by the second term in Eq. (4), i.e.,  $\mathbf{v}_d = -(3\mu_\alpha/4\pi\mu_0 r_\alpha^5)\mathbf{r}_\alpha[\mathbf{r}_\alpha \mathbf{r}_\alpha : \nabla \mathbf{v}_0(\mathbf{x}_\alpha)]$ . The vorticity due to this disturbance flow is  $\boldsymbol{\omega} = [\nabla \times \mathbf{v}_d]/2$ . All calculations done, the vorticity at the center of the sphere reflected by the Stokeslet is found to be zero (see SM [21]). Only the flow due to the source dipole creates a nonzero vorticity around the sphere. The torque-free condition requires the angular velocity of the sphere  $\boldsymbol{\Omega}$  to be equal to the

vorticity,

$$\boldsymbol{\Omega} = \boldsymbol{\omega} = -\frac{9\mu_\alpha a^3}{16\pi\mu_0 d_\alpha^7} \hat{\boldsymbol{d}}_\alpha \times \boldsymbol{U} + O(\mu_\alpha^2 a^3 / \mu_0^2 d_\alpha^9), \quad (7)$$

where the next correction comes from the vorticity of the flow field arising from reflection of the Stokeslet. The translational velocity of the sphere is attached to the body and rotates with it while the viscosity sink is fixed in space, representing a viscosity gradient in space or produced by local heating of fluid. In the steady state,  $\hat{\boldsymbol{d}}_\alpha$  and  $\boldsymbol{U}$  become antiparallel to each other. Hence, the active particle performs positive *viscotaxis*, i.e., it translates towards regions of higher viscosity [24].

We then introduce multiple viscosity sinks arranged in a hemispherical shell at  $\boldsymbol{x} = \boldsymbol{d}_\alpha$ , around one side of the sphere centered at the origin, so that  $\boldsymbol{d}_\alpha = d_\alpha [\sin \theta \cos \phi, \sin \theta \sin \phi, \cos \theta]$ , where  $\theta$  and  $\phi$  are the polar and azimuthal angles, respectively. We also define an effective viscosity gradient  $\nabla\mu$  making an angle with  $\Theta$  with  $\boldsymbol{U}$  [see Fig. 2(a)]. The individual contributions of the viscosity sinks are easily summed to find the net rotational velocity of the sphere,

$$\Omega_y = -\beta \sin \Theta, \quad (8)$$

where

$$\beta = \frac{9a^3 \mu_\alpha U}{16\pi \mu_0 d_\alpha^7} \left[ 1 + \frac{N_\phi}{2} \left( \cot \frac{\pi}{4N_\theta} - 1 \right) \right], \quad (9)$$

and  $N_{\theta,\phi}$  are the total number of viscosity sinks along the polar and azimuthal directions such that  $\theta \in [0, \pi/2)$  and  $\phi \in [0, 2\pi)$ . The equation  $\partial_t \Theta = -\Omega_y$  is integrated in time to obtain

$$\Theta(t) = 2 \tan^{-1} [\tan\{\Theta(0)/2\} \exp(\beta t)]. \quad (10)$$

The angle  $\Theta(t)$  is plotted in Fig. 2(b) for varying  $d_\alpha^* = d_\alpha/a = 1 - 2$  with 57 identical viscosity sinks of strength  $\mu_\alpha = -0.01\mu_0$  arranged around the particle in a hemisphere. It matches exactly with the numerical solution obtained by integrating  $\boldsymbol{U}$  in time as it rotates with  $\boldsymbol{\Omega}$  (see SM [21] for validation). For a given  $N_\theta$ , and area density of viscosity sinks,  $n = [N_\phi(N_\theta - 1) + 1]/4\pi d_\alpha^{*2}$ , we plot  $\Omega_y$  as a function of  $d_\alpha^*$  for a few different area densities in Fig. 2(c). Unsurprisingly, while  $\Omega_y$  due to a single viscosity sink varies as  $1/d_\alpha^{*7}$  according to Eq. (7), integrating the contribution due to multiple sinks arranged in a hemispherical shell results in  $\Omega_y \propto 1/d_\alpha^{*5}$ .

We compare the results from the point viscosity model with a paper that considered the effect of viscosity gradients, generated by temperature gradients, on the motion of rigid particles. Oppenheimer *et al.* [14] showed that the translational and rotational velocities of a Janus hot spherical particle get coupled due to the difference in viscosities around its surface. The hot side of the particle heats the fluid surrounding it and decreases its viscosity, thereby creating a viscosity gradient. The Faxen laws for a sphere in a fluid with a weakly varying linear viscosity gradient,  $\mu(\boldsymbol{x}) = \mu_0 + \epsilon \boldsymbol{x} \cdot \nabla\mu$ , were found to be  $\boldsymbol{F} = -6\pi\mu_0 a \boldsymbol{U} + \epsilon 2\pi a^3 \nabla\mu \times \boldsymbol{\Omega}$  and  $\boldsymbol{L} = -8\pi\mu_0 a^3 \boldsymbol{\Omega} - \epsilon 2\pi a^3 \nabla\mu \times \boldsymbol{U}$ . The angular velocity of a translating sphere is easily found from the torque-free condition by substituting  $\boldsymbol{L} = \mathbf{0}$  to obtain

$$\boldsymbol{\Omega} = -(\epsilon/4\mu) \nabla\mu \times \boldsymbol{U} + O(\epsilon^2). \quad (11)$$

Equation (11) has the same functional form as Eq. (7) for  $\mu_\alpha < 0$  and  $\boldsymbol{d}_\alpha = -\nabla\mu$ . Consequently, it was shown that a torque-free translating sphere rotates such that its translational velocity vector will align with the viscosity gradient vector in the steady state which is consistent with our findings. Hence, we are able to obtain the same physics as Oppenheimer *et al.* [14] by modeling hot fluid around the sphere as concentrated viscosity sinks. Remarkably, the method of point viscosities can be used to create an arbitrary spatial viscosity distribution and applied to any arbitrary shaped particle. This method may be applied to other problems such as a squirmer [25,26] or a phoretic particle [27] in which case the leading flow field is that generated by a stresslet itself.

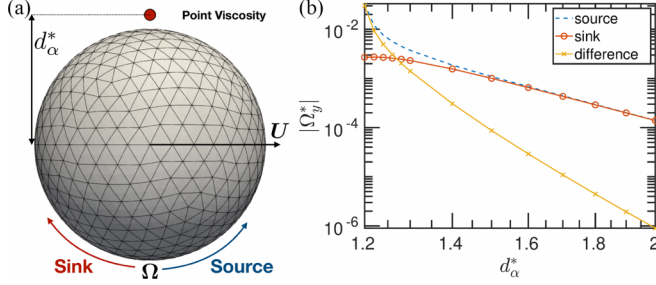


FIG. 3. Log-log plot of the absolute value of the angular velocity  $|\Omega_y^*|$  of a translating spherical particle in the presence of a viscosity source (blue dashed) and sink (red circle) of strength  $\mu_\alpha = \pm 0.1\mu_0$ , solved using the boundary element method as a function of the distance between the sphere center and the point viscosity, denoted as  $d_\alpha^*$ . The difference between the magnitude of the angular velocities due to the source and sink (yellow cross) is seen to decrease as they move farther away from the sphere's surface.

The effect of a single point viscosity on the angular velocity of a translating sphere may appear weak due to its  $1/d_\alpha^{*7}$  dependency because the disturbance vorticity has been calculated at the center of the sphere using the far-field assumption. In order to explore the effect of a point viscosity accurately on the hydrodynamics of a rigid particle, including near-field effects, we perform simulations based on the boundary element method [28,29]. The point viscosity now interacts with the entire surface of the particle. The boundary integral equation relevant for a Stokes equation with variable viscosity was derived by Pozrikidis using the reciprocal theorem [30]. The area integral involving variable viscosity was solved numerically in two dimensions. For a point viscosity in space, the equations simplify considerably (see SM [21]). The velocity field due to a translating and rotating rigid particle in the presence of point viscosities is written succinctly in the form of an integral equation,

$$\mathbf{v}(\mathbf{x}_0) = -\frac{1}{8\pi\mu_0} \iint_S \mathbf{f}(\mathbf{x}, \mathbf{x}_\alpha) \cdot \mathbf{G}_{\text{mod}}(\mathbf{x}, \mathbf{x}_0, \mathbf{x}_\alpha) dS(\mathbf{x}), \quad (12)$$

where  $\mathbf{x}_0 \neq \mathbf{x}_\alpha$  is an evaluation point anywhere in the fluid domain,  $\mathbf{x} \in S$  is the integration point on the sphere's surface,  $\mathbf{G}_{\text{mod}} = \mathbf{G} - \mathbf{G}_v$  is the modified Green's function,  $\mathbf{G}$  is the Oseen-Burgers tensor,  $G_{v,lj} = (\mu_\alpha/8\pi\mu_0)T_{ijk}(\mathbf{x}_\alpha, \mathbf{x}_0)[\nabla_{y,i}G_{lk}(\mathbf{x}, \mathbf{y})]_{y=\mathbf{x}_\alpha}$  is the Green's function due to a point viscosity, and  $\mathbf{T}(\mathbf{x}_\alpha, \mathbf{x}_0) = -6\mathbf{p}\mathbf{p}\mathbf{p}/p^5$  is the stresslet, with  $\mathbf{p} = \mathbf{x}_\alpha - \mathbf{x}_0$ . The surface velocity is  $\mathbf{v}(\mathbf{x}) = \mathbf{U} + \boldsymbol{\Omega} \times (\mathbf{x} - \mathbf{x}_c)$  and  $\mathbf{f}$  is the hydrodynamic traction acting on the body.

We again consider the hydrodynamics of a torque-free translating sphere and find its rotational velocity due to the presence of a point viscosity [see Fig. 3(a)]. The viscous force and torque acting on the sphere are found by integrating the hydrodynamic tractions after solving Eq. (12) numerically by discretizing the sphere's surface into triangular elements [28,29],  $\mathbf{F} = \iint_S \mathbf{f} dS(\mathbf{x})$ ,  $\mathbf{L} = \iint_S (\mathbf{x} - \mathbf{x}_c) \times \mathbf{f} dS(\mathbf{x})$ . The sphere is centered at the origin,  $\mathbf{x}_c = \mathbf{0}$ , and the point viscosity is placed at a distance  $d^* = (0, 0, d_\alpha^*)$ , scaled by the sphere radius  $a$ . The magnitude of the angular velocity of the sphere,  $|\boldsymbol{\Omega}| = |\mathbf{L}/8\pi\mu_0 a^3|$ , is plotted for the case of a single isolated viscosity sink and source in Fig. 3(b). Here, we make a curious observation. The angular velocities due to a viscosity sink and source are found to be in the positive and negative  $y$  directions, respectively, as expected. However, their magnitudes are not the same when  $d_\alpha^* < 1.5$ . This is in contrast to both the results of Oppenheimer *et al.* [14], Eq. (11), and the far-field result derived in this paper, Eq. (7), wherein switching the direction of the viscosity gradient or changing a sink into a source simply changes the direction of the angular velocity, while its magnitude remains unchanged. This difference arises because both Eqs. (11) and (7) only consider the leading-order viscosity gradient and point viscosity effects, respectively. In contrast, in the numerical simulations, the point viscosity interacts nonlinearly with the sphere's surface. As a result, the magnitudes of the angular velocities approach each

other only when  $\|\mathbf{G}_v\|$  becomes sufficiently small compared to  $\|\mathbf{G}\|$ , i.e., when the point viscosity is far away from the surface or sufficiently weak in magnitude. This is easily seen by considering two cases: the hydrodynamics of a sphere placed next to a viscosity source (subscript 1) and a sink (subscript 2). The resulting system of linear equations arising from Eq. (12) for these two cases is  $\mathbf{f}_1 = (\mathbf{G} - \mathbf{G}_v)^{-1}\mathbf{v}$ ,  $\mathbf{f}_2 = (\mathbf{G} + \mathbf{G}_v)^{-1}\mathbf{v}$ , where the vectors  $\mathbf{v}$ ,  $\mathbf{f}_{1,2}$  denote the surface velocity and traction values on the discretized sphere and  $\mathbf{G}$  denotes the Green's function matrix. Integrating the tractions gives us the hydrodynamic torque  $\mathbf{L}_{1,2} = \iint_S (\mathbf{x} - \mathbf{x}_c) \times [(\mathbf{G} \pm \mathbf{G}_v)^{-1}\mathbf{v}] dS(\mathbf{x})$ . Noting that  $\iint_S (\mathbf{x} - \mathbf{x}_c) \times \mathbf{G}^{-1}\mathbf{v} dS(\mathbf{x}) = \mathbf{0}$ , and performing a Taylor series expansion of  $\mathbf{L}_{1,2}$ , we find  $\mathbf{L}_1 \rightarrow -\mathbf{L}_2$ , as  $\mathbf{G}^{-1}\mathbf{G}_v$  becomes smaller, thereby explaining the conundrum.

In this Letter, we proposed a method to model viscosity heterogeneities in a fluid shrunk to a point. We found the disturbance flow field due to these point viscosity variations to be the same as that due to a stresslet, written as a singularity solution. A wide variety of physical problems such as potential flow, electrostatics, linear elasticity, and wave propagation are amenable to theoretical analysis because their governing equations admit singularity solutions. Hence, the ideas presented here may be applied to these other physical phenomena as well when material heterogeneities are present in the media. The modeling framework developed in this Letter opens up several different avenues of research. One such avenue is modeling generalized non-Newtonian fluids relevant for problems in biology [31] such as bacteria locomotion or beating cilia [32]. To solve such problems, the point viscosities' strength can be made to depend on time or the velocity gradients, while avoiding discretization of the entire fluid domain. For example, it has been hypothesized that the gastric pathogen *H. pylori* can propel itself through the mucus gel by reducing its viscoelasticity and attach to epithelial cells [33]. Theoretical models to understand this phenomenon have been developed based on Taylor's swimming sheet in a phase-separated fluid [34] and in a layer of Newtonian fluid bounded by a Brinkman fluid [35]. Using the point viscosity model, solving the hydrodynamics of a three-dimensional model of a bacterium swimming [36,37] in a heterogeneous fluid becomes feasible.

Recent papers have considered the effect of viscosity gradients on swimming microorganisms such as green algae [38,39] and model active swimmers [40,41]. Incorporating the effect of point viscosities in such model swimmers will yield further physical insight into how microorganisms respond to viscosity variations in environments where they live. Also, the effect of nonlinear interactions between multiple point viscosities on a particle's motion has been neglected here, and may have nontrivial consequences. Finally, the point viscosities may be made to diffuse in time and advect with the velocity field, thereby relaxing the quasistatic assumption.

We thank D. Pritchard for helpful suggestions and comments.

- 
- [1] S. Chien, Biophysical behavior of red cells in suspensions, in *Red Blood Cell*, edited by D. M. Surgenor (Academic, New York, 1975), Vol. 2, pp. 1031–1133.
  - [2] C.-H. Heldin, K. Rubin, K. Pietras, and A. Östman, High interstitial fluid pressure—an obstacle in cancer therapy, *Nat. Rev. Cancer* **4**, 806 (2004).
  - [3] R. K. Jain and T. Stylianopoulos, Delivering nanomedicine to solid tumors, *Nat. Rev. Clin. Oncol.* **7**, 653 (2010).
  - [4] C. P. Brangwynne, C. R. Eckmann, D. S. Courson, A. Rybarska, C. Hoegel, J. Gharakhani, F. Jülicher, and A. A. Hyman, Germline P granules are liquid droplets that localize by controlled dissolution/condensation, *Science* **324**, 1729 (2009).
  - [5] C. P. Brangwynne, T. J. Mitchison, and A. A. Hyman, Active liquid-like behavior of nucleoli determines their size and shape in *Xenopus laevis* oocytes, *Proc. Natl. Acad. Sci. USA* **108**, 4334 (2011).
  - [6] A. A. Hyman, C. A. Weber, and F. Jülicher, Liquid-liquid phase separation in biology, *Annu. Rev. Cell Dev. Biol.* **30**, 39 (2014).

- [7] L. G. Leal, The motion of small particles in non-Newtonian fluids, *J. Non-Newtonian Fluid Mech.* **5**, 33 (1979).
- [8] R. B. Bird, R. C. Armstrong, and O. Hassager, *Dynamics of Polymeric Liquids, Volume 1: Fluid Mechanics* (Wiley, New York, 1987).
- [9] J. R. A. Pearson, Variable-viscosity flows in channels with high heat generation, *J. Fluid Mech.* **83**, 191 (1977).
- [10] H. Ockendon and J. R. Ockendon, Variable-viscosity flows in heated and cooled channels, *J. Fluid Mech.* **83**, 177 (1977).
- [11] H. Ockendon, Channel flow with temperature-dependent viscosity and internal viscous dissipation, *J. Fluid Mech.* **93**, 737 (1979).
- [12] A. Hooper, B. R. Duffy, and H. K. Moffatt, Flow of fluid of non-uniform viscosity in converging and diverging channels, *J. Fluid Mech.* **117**, 283 (1982).
- [13] S. Morris, The effects of a strongly temperature-dependent viscosity on slow flow past a hot sphere, *J. Fluid Mech.* **124**, 1 (1982).
- [14] N. Oppenheimer, S. Navardi, and H. A. Stone, Motion of a hot particle in viscous fluids, *Phys. Rev. Fluids* **1**, 014001 (2016).
- [15] M. Mittasch, P. Gross, M. Nestler, A. W. Fritsch, C. Iserman, M. Kar, M. Munder, A. Voigt, S. Alberti, S. W. Grill, and M. Kreysing, Non-invasive perturbations of intracellular flow reveal physical principles of cell organization, *Nat. Cell Biol.* **20**, 344 (2018).
- [16] W. Liao, E. Erben, M. Kreysing, and E. Lauga, Theoretical model of confined thermoviscous flows for artificial cytoplasmic streaming, *Phys. Rev. Fluids* **8**, 034202 (2023).
- [17] H. Lamb, *Hydrodynamics* (Cambridge University Press, Cambridge, UK, 1932).
- [18] J. Happel and H. Brenner, *Low Reynolds Number Hydrodynamics: With Special Applications to Particulate Media* (Springer, Berlin, 2012).
- [19] S. Kim and S. J. Karrila, *Microhydrodynamics: Principles and Selected Applications* (Courier Corporation, North Chelmsford, MA, 2013).
- [20] M. J. Lighthill, *An Introduction to Fourier Analysis and Generalised Functions* (Cambridge University Press, Cambridge, UK, 1958).
- [21] See Supplemental Material at <http://link.aps.org/supplemental/10.1103/PhysRevFluids.8.L051301> for the detailed derivation of Eqs. (3), (4), (6), (10), and (11) and an illustrative example of how to capture the hydrodynamic interaction between point viscosities, which includes Ref. [22].
- [22] M. Lisicki, Four approaches to hydrodynamic Green's functions—the Oseen tensors, [arXiv:1312.6231](https://arxiv.org/abs/1312.6231).
- [23] G. I. Taylor, The viscosity of a fluid containing small drops of another fluid, *Proc. R. Soc. London, Ser. A* **138**, 41 (1932).
- [24] M. G. Petrino and R. N. Doetsch, ‘Viscotaxis’, a new behavioural response of *Leptospira interrogans (biflexa)* strain B16, *J. Gen. Microbiol.* **109**, 113 (1978).
- [25] M. J. Lighthill, On the squirming motion of nearly spherical deformable bodies through liquids at very small Reynolds numbers, *Commun. Pure Appl. Math.* **5**, 109 (1952).
- [26] J. R. Blake, A spherical envelope approach to ciliary propulsion, *J. Fluid Mech.* **46**, 199 (1971).
- [27] J. R. Howse, R. A. L. Jones, A. J. Ryan, T. Gough, R. Vafabakhsh, and R. Golestanian, Self-Motile Colloidal Particles: From Directed Propulsion to Random Walk, *Phys. Rev. Lett.* **99**, 048102 (2007).
- [28] C. Pozrikidis, *Boundary Integral and Singularity Methods for Linearized Viscous Flow* (Cambridge University Press, Cambridge, UK, 1992).
- [29] C. Pozrikidis, *A Practical Guide to Boundary Element Methods with the Software Library BEMLIB* (Chapman & Hall/CRC, Boca Raton, FL, 2002).
- [30] C. Pozrikidis, Reciprocal identities and integral formulations for diffusive scalar transport and Stokes flow with position-dependent diffusivity or viscosity, *J. Eng. Math.* **96**, 95 (2016).
- [31] E. Lauga and T. R. Powers, The hydrodynamics of swimming microorganisms, *Rep. Prog. Phys.* **72**, 096601 (2009).
- [32] N. Pellicciotta, D. Das, J. Kotar, M. Faucourt, N. Spassky, E. Lauga, and P. Cicuta, Cilia density and flow velocity affect alignment of motile cilia from brain cells, *J. Expt. Biol.* **223**, jeb229310 (2020).

- [33] J. P. Celli, B. S. Turner, N. H. Afdhal, S. Keates, I. Ghiran, C. P. Kelly, R. H. Ewoldt, G. H. McKinley, P. So, S. Erramilli, and R. Bansil, *Helicobacter pylori* moves through mucus by reducing mucin viscoelasticity, [Proc. Natl. Acad. Sci. USA](#) **106**, 14321 (2009).
- [34] Y. Man and E. Lauga, Phase-separation models for swimming enhancement in complex fluids, [Phys. Rev. E](#) **92**, 023004 (2015).
- [35] S. A. Mirbagheri and H. C. Fu, *Helicobacter pylori* Couples Motility and Diffusion to Actively Create a Heterogeneous Complex Medium in Gastric Mucus, [Phys. Rev. Lett.](#) **116**, 198101 (2016).
- [36] D. Das and E. Lauga, Computing the motor torque of *Escherichia coli*, [Soft Matter](#) **14**, 5955 (2018).
- [37] D. Das and E. Lauga, Transition to bound states for bacteria swimming near surfaces, [Phys. Rev. E](#) **100**, 043117 (2019).
- [38] M. R. Stehnach, N. Waisbord, D. M. Walkama, and J. S. Guasto, Viscophobic turning dictates microalgae transport in viscosity gradients, [Nat. Phys.](#) **17**, 926 (2021).
- [39] S. Coppola and V. Kantsler, Green algae scatter off sharp viscosity gradients, [Sci. Rep.](#) **11**, 399 (2021).
- [40] B. Liebchen, P. Monderkamp, B. ten Hagen, and H. Löwen, *Viscotaxis*: Microswimmer Navigation in Viscosity Gradients, [Phys. Rev. Lett.](#) **120**, 208002 (2018).
- [41] C. Datt and G. J. Elfring, Active Particles in Viscosity Gradients, [Phys. Rev. Lett.](#) **123**, 158006 (2019).